Fermi National Accelerator Laboratory

FERMI-PUB-89/127-T
Submitted to Physical Review D
July 17, 1989

Minimal Dynamical Symmetry Breaking of the Standard Model

William A. Bardeen
Christopher T. Hill
Manfred Lindner

Fermi National Accelerator Laboratory
P.O. Box 500, Batavia, Illinois, 60510

Abstract

We formulate the dynamical symmetry breaking of the Standard Model by a top quark condensate in analogy with BCS theory. The low energy effective Lagrangian is the usual Standard Model to leading order in a fermion planar-loop approximation, with supplemental relationships connecting masses of top quark, W boson, and the Higgs boson which now appears as a $\bar{t}t$ boundstate. Precise predictions for m_{top} and m_{Higgs} are obtained by abstracting the compositeness condition for the Higgs boson to boundary conditions on the renormalization group equations for the full Standard Model at high energy.

Operated by Universities Research Association Inc. under contract with the United States Department of Energy

I. Introduction

The top quark is now known to be more massive than 60 GeV within the context of the Standard Model. Therefore, its coupling to the elementary Higgs scalar is large, at least of order g_2 the $SU(2)$ gauge coupling constant at low energies, and possibly larger. Strong coupling suggests that the symmetry breakdown of the Standard Model may be a dynamical mechanism which intimately involves the top quark, and several authors [1,2], most notably Nambu [1], have recently experimented with this idea. Essentially one implements a BCS or Nambu–Jona-Lasinio mechanism in which a new fundamental interaction associated with a high energy scale, Λ, is used to trigger the formation of a low energy condensate, $\langle \bar{t}_L t_R \rangle$. The bootstrapping of the symmetry breaking mechanism to the top quark introduces no fundamental Higgs scalar bosons and, by virtue of its economy, leads to new predictions which are in principle testable, or which constrain or rule out the mechanism altogether. In particular, we are able to derive predictions for m_{top} and m_{Higgs} in this scheme.

This is the minimal conceivable dynamical breaking of the Standard Model in terms of the relevant number of field degrees of freedom, in which we treat the gauge bosons as fundamental. The usual Cabibbo–Kobayashi–Maskawa structure and fermion mass spectrum is readily accomodated, but *bona fide predictions* of mixing angles and light quark masses are not derivable until one specifies the dynamics at the scale Λ more precisely. The usual one–Higgs–doublet Standard Model emerges as the low energy effective Lagrangian, but with new constraints that lead to nontrivial predictions.

We begin with an analysis of the gauged Nambu–Jona-Lasinio mechanism [3] applied to the Standard Model, within the approximation of keeping only the effects of the fermionic determinant as described below. This yields the "bare" mass relationships, but the most important new results which emerge are the compositeness

conditions pertaining to the Higgs boson boundstate, with an otherwise conventional low energy effective Lagrangian for the Standard Model. We translate these conditions into boundary conditions at the scale Λ on the renormalization group equations *for the full theory*, which now includes the effects of gauge boson and Higgs boson loops, *etc.* Certain renormalization group trajectories are thereby associated with the existence of composite structure. These lead to precise predictions for m_{top} and m_{Higgs}, which are very insensitive to the scale of new physics, Λ.

We show that the compositeness condition is the statement that the induced wave–function renormalization constant, Z_H, for the Higgs field H must vanish at the scale Λ. It is just this condition, coupled to our demand for a symmetry breaking solution to the theory at low energies, which enables one to "predict" the mass of the top quark and the mass of the dynamical scalar Higgs boson. The composite theory is effectively a strongly coupled (Higgs–Yukawa and quartic Higgs couplings) Standard Model at the scale Λ. The low energy predictions that emerge are governed by infra–red renormalization group fixed–points [4,5]. The top quark is predicted to lie near 230 GeV for $\Lambda \sim 10^{15}$ GeV. We discuss in some detail the consistency of these predictions with the collection of experimental results that constitute the so–called ρ parameter bound, and we conclude that *it is premature to rule out top quark masses as high as* ~ 260 *to* ~ 280 GeV.

Our preliminary goal is to make precise the definition of the minimal dynamical symmetry breaking scheme beginning with a well–defined quantum field theory at the scale Λ. We imagine that at some high energy scale, Λ, the Standard Model contains only the usual quark, lepton and gauge boson degrees of freedom, but no fundamental Higgs scalar. We then introduce a new effective four–fermion vertex with coefficient, G, of order $1/\Lambda^2$. This interaction must, of course, be electroweak gauge invariant. If we consider, for discussion, the approximation in which all quarks and leptons other

than the top quark are massless we may then define the theory at the scale Λ to be:

$$L = L_{kinetic} + G(\bar{\Psi}^i_L t_R \bar{t}_R \Psi_{iL}) \tag{1.1}$$

where i runs over $SU(2)$ indices and $L_{kinetic}$ contains the usual gauge invariant fermion and gauge boson kinetic terms, but there is no Higgs field in L. The model readily generalizes to a more realistic mass spectrum, as well as a multiple effective Higgs doublet scheme as described below in Section III.

We first consider a solution based upon the effects of the fermionic determinant alone, *i.e.*, a fermion bubble approximation. This is equivalent to a large–N_{color} expansion in the limit in which the QCD coupling constant is set to zero, and it captures nonperturbative features of the theory from the point of view of a small–coupling constant expansion. We demand a self–consistent dynamical solution to the gap equation for the mass of the top quark, given in terms of an induced vacuum matrix element of the form $\langle \bar{t}t \rangle$. This will generate poles in the scalar and pseudoscalar channels, corresponding to a physical state with a mass of $2m_t$ and zero–mass Goldstone bosons, respectively. From the vector boson vacuum polarization analysis we determine the electroweak vector boson masses in terms of the top quark mass. Moreover, we will see that the low energy induced Lagrangian has all of the renormalization properties, and is indistinguishable from, the Standard Model with a single Higgs doublet. The essential results of this analysis are presented in Section II, while the full technical details are given in Appendices A and B.

The central result is that the physical Higgs boson is composite and the top quark and Higgs boson masses become related to the observable electroweak scale. Here we do not address the usual problem of the gauge hierarchy, *i.e.*, how we can naturally maintain the hierarchy of scales $M_W << \Lambda$. It should be noted, however, that the quadratic divergence fine–tuning problem is isolated in the gap equation sector of this analysis; once the gap equation is satisfied for a symmetry breaking scale of order

M_W, there is no further fine–tuning needed.

We emphasize that the predictions of the fermionic determinant analysis are inherently limited. The discussion of this approximation will be presented in Section II, but we emphasize that it is intended only as a schematic for the full theory, *i.e.*, the fermionic determinant analysis should be viewed only as a model discussion of the actual physical situation. It neglects, *e.g.*, radiative corrections due to gauge bosons and propagation of the composite Higgs boson itself. It is only upon abstracting the compositeness conditions to the full theory that we obtain reliable predictions for m_{top} and m_{Higgs}.

Thus we begin in Section II with a digest of the fermionic determinant analysis, with the full technical details given in Appendix A and B. In Section III we write the effective Lagrangian in terms of the induced low energy composite particles. In Section IV we present the analysis of the full theory and give precise results that include all of the effects in the Standard Model. We discuss the viability of the results in light of the most stringent limits on m_{top} from the "ρ parameter" analysis in Section IV.B. In Section V we present our conclusions and compare our results to other recent works.

II. Fermionic Determinant Approximation

The present discussion summarizes how the dynamical symmetry breaking mechanism through top quark condensation works in the approximation of keeping only fermionic loops, or, equivalently, to leading order in $1/N_c$ with the QCD coupling constant set to zero. This section is mostly a digest of results, and a more detailed discussion is given in Appendix A & B. We presently ignore all gauge boson and composite–Higgs boson radiative corrections. The "bare" relationships emerge between the composite Higgs boson, top quark and W boson masses. These relationships are only approximate, and in Section IV we will give the precise predictions, after abstracting the compositeness conditions to the full theory.

A. Gap Equation

We will begin by summing the planar bubble diagrams in which the four–fermion interaction of eq.(1.1) is iterated. We first consider the solution to the gap equation for the induced top quark mass. This is indicated as in Fig.(1):

$$m_t = -\frac{1}{2}G\langle\bar{t}t\rangle \tag{2.1}$$

$$= 2GN_c m_t \frac{i}{(2\pi)^4}\int d^4l\,(l^2-m_t^2)^{-1} \tag{2.2}$$

The result of evaluating eq.(2.2) with a momentum space cut–off Λ is:

$$G^{-1} = \frac{N_c}{8\pi^2}\left(\Lambda^2 - m_t^2\ln(\Lambda^2/m_t^2)\right). \tag{2.3}$$

Here, we regard G and Λ as fundamental parameters of the theory and we solve for m_t. Normally, for very large Λ, perhaps of order the GUT scale 10^{15} GeV, we would expect the solution of this equation to produce a large mass, $m_t \sim \Lambda$ in the broken

symmetry phase. We see that a solution for $m_t \sim M_W$ for such large Λ constitutes a fine–tuning problem in that $G^{-1} - N_c\Lambda^2/8\pi^2$ must then be very small. This is, indeed, the usual fine–tuning or gauge hierarchy problem of the Standard Model. The gap equation contains a quadratic divergence, corresponding to the usual Higgs mass quadratic divergence in the Standard Model. However, the fine–tuning problem will be isolated in the gap equation, *i.e.*, once we tune G to admit the desirable solution to any given order in $1/N_c$, we need cancel no other quadratic divergences in other amplitudes.

B. Scalar and Goldstone Modes

Let us now assume that the parameters, G, Λ admit a solution for m_t to the gap equation, eq.(2.3). We now consider the sum of scalar channel fermion bubbles of Fig.(2) generated by the interaction eq.(1.1):

$$\Gamma_s(p^2) = -\frac{1}{2}G - (\frac{1}{2}G)^2 i \int d^4x\, e^{ipx} \langle T\, \bar{t}t(0)\, \bar{t}t(x)\rangle_{connected} + ... \qquad (2.4)$$

A useful technical trick for evaluating this amplitude while simultaneously implementing the gap equation is given in Appendix A. The result is:

$$\Gamma_s(p^2) = \frac{1}{2N_c}\left[(p^2 - 4m_t^2)(4\pi)^{-2}\int_0^1 dx \log\left\{\Lambda^2/(m_t^2 - x(1-x)p^2)\right\}\right]^{-1} \qquad (2.5)$$

Γ_s is the propagator for the dynamically generated boundstate, a scalar composite of $\bar{t}t$. In particular, owing to the pole at $p^2 = 4m_t^2$, we see that the theory predicts a scalar boundstate with a mass of $2m_t$ [1]. This is a standard result quoted for the Nambu–Jona-Lasinio model. We emphasize that this is the physical, observable, low energy Higgs boson, and that the prediction holds only to leading order in $1/N_c$ in the absence of gauge boson corrections.

This physical particle is a boundstate of $\bar{t}t$, arising by the attractive four-fermion interaction at the scale Λ of eq.(1.1). It is a loosely bound state, since it lies on top of the threshold for open $\bar{t}t$ and has vanishing binding energy to this order. The prediction cannot be viewed at this stage as a very precise one. In fact, the essential point is that this is a composite Higgs boson model and we will give a more precise determination of its mass in Section IV upon considering the full renormalization group behavior of the theory.

Notice, furthermore, that solutions exist to eq.(2.3) only for positive G^{-1}, *i.e.*, for attractive interactions only. Though the interactions at the high energy scale Λ are attributed to new physics, from the point of view of the low energy physics the composite Higgs boson may be viewed as generating the effective interactions. At high energy scales approaching Λ, the composite boson mass-squared is of order G^{-1} and is non-propagating. As we evolve to the low energy scales by integrating out the fermion loops we will find the composite boson develops a negative mass-squared, $m_H^2 \propto G^{-1} - N_c\Lambda^2/8\pi^2 < 0$ from eq.(2.3), and a spontaneous symmetry breaking occurs.

Since the mechanism is a dynamical breaking of the continuous $SU(2) \times U(1)$ symmetry, it must imply the existence of Goldstone modes. Moreover, the symmetry breaking transforms as $I = \frac{1}{2}$ and will produce the same spectrum of Goldstone bosons as in the Standard Model Higgs-sector. A Goldstone pole thus appears in the bubble sum for the neutral pseudo-scalar channel:

$$\Gamma_p(p^2) = -\frac{1}{2}G - (\frac{1}{2}G)^2 i \int d^4x\, e^{ipx} \langle T\, \bar{t}\gamma_5 t(0)\, \bar{t}\gamma_5 t(x)\rangle_{connected} + \ldots \qquad (2.6)$$

By similar manipulations as in eq.(2.5) and use of the gap equation we find the result:

$$\Gamma_p(p^2) = \frac{1}{2N_c}\left[(p^2)(4\pi)^{-2}\int_0^1 dx\, \log\left\{\Lambda^2/(m_t^2 - x(1-x)p^2)\right\}\right]^{-1} \qquad (2.7)$$

and the Goldstone pole at $p^2 = 0$ is seen to occur explicitly.

Moreover, charged Goldstone modes appear in the flavored channels corresponding to the quantum numbers of the W boson:

$$\Gamma_F = -\frac{1}{4}G - (\frac{1}{4}G)^2 i \int d^4x\ e^{ipx} \left\langle T\ \bar{b}(1+\gamma_5)t(0)\ \bar{t}(1-\gamma_5)b(x)\right\rangle_{connected} + \ldots \quad (2.8)$$

whence:

$$\Gamma_F(p^2) = \frac{1}{8N_c}\left[(p^2)(4\pi)^{-2}\int_0^1 dx(1-x)\log\left\{\Lambda^2/((1-x)m_t^2 - x(1-x)p^2)\right\}\right]^{-1} \quad (2.9)$$

where we have assumed $m_b \approx 0$.

C. Vector Bosons

Thus far we have considered only a conventional Nambu–Jona-Lasinio model for the symmetry group $SU(2)\times U(1)$ in the absence of gauge fields. Now let us consider the model with the gauge coupling constants restored. Of course, we have a dynamical Higgs–mechanism and the gauge bosons acquire masses by "eating" the dynamically generated Goldstone poles. We obtain a second prediction of the theory in the form of a relation between the W boson mass and the top quark mass.

Consider now the inverse propagator of the gauge bosons. We rescale fields to bring the gauge coupling constants into the gauge boson kinetic terms, *i.e.*, we write the kinetic terms in the form $(1/4g^2)(F_{\mu\nu})^2$. We are not integrating over the gauge boson fields and need specify no gauge fixing at this stage. Thus, for the W boson we have:

$$\frac{1}{g_2^2}D^W_{\mu\nu}(p)^{-1} = \frac{1}{g_2^2}(p^\mu p^\nu - g^{\mu\nu}p^2) + \frac{i}{2}\int d^4x\ \left\langle T\ \bar{t}_L\gamma_\mu b_L(0)\ \bar{b}_L\gamma_\nu t_L(x)\right\rangle \quad (2.10)$$

where g_2 is the $SU(2)$ coupling constant. For the T–ordered product we again expand in the interaction Lagrangian of eq.(1.1) and sum the planar bubbles, Fig.(3). We

assume the top quark has a mass satisfying eq.(2.3), and the gap equation is satisfied in the loop expansion, which maintains the gauge invariance. This sum can thus be written in terms of the flavor bubbles evaluated in eq.(2.9) (see Appendix A).

It is useful to write the induced inverse W boson propagator in the form:

$$\frac{1}{g_2^2} D^W_{\mu\nu}(p)^{-1} = (p_\mu p_\nu/p^2 - g_{\mu\nu}) \left[\frac{1}{\bar{g}_2^2(p^2)} p^2 - \bar{v}^2(p^2) \right] . \tag{2.11}$$

The W boson mass is the solution to the the mass–shell condition:

$$M_W^2 = p^2 = \bar{g}_2(p^2)^2 \bar{v}^2(p^2) \tag{2.12}$$

while the Fermi constant is the zero–momentum expression:

$$G_F = \frac{1}{8\bar{v}(0)^2} \tag{2.13}$$

In the bubble approximation we find:

$$\begin{aligned} \frac{1}{\bar{g}_2^2(p^2)} &= \frac{1}{g_2^2} + N_c(4\pi)^{-2} \int_0^1 dx\ 2x(1-x) \\ &\qquad \times \log \left\{ \Lambda^2/(xm_b^2 + (1-x)m_t^2 - x(1-x)p^2) \right\} \end{aligned} \tag{2.14}$$

and:

$$\begin{aligned} \bar{v}(p^2) &= N_c(4\pi)^{-2} \int_0^1 dx\ (xm_b^2 + (1-x)m_t^2) \\ &\qquad \times \log \left\{ \Lambda^2/(xm_b^2 + (1-x)m_t^2 - x(1-x)p^2) \right\} \end{aligned} \tag{2.15}$$

At this stage of the approximation it is useful to note the quantitative result for m_t in terms of G_F. Eq. (2.13) combined with eq.(2.15) gives:

$$\bar{v}^2(0) = \frac{1}{8G_F} \approx N_c(4\pi)^{-2} \int_0^1 (1-x) m_t^2 \log \left\{ \Lambda^2/((1-x)m_t^2) \right\}$$

$$\approx \frac{1}{2} N_c (4\pi)^{-2} m_t^2 \log\{\Lambda^2/m_t^2\} \tag{2.16}$$

For example, with $\Lambda = 10^{15}$ GeV one finds $m_t \approx 160$ GeV.

To what extent is this an accurate prediction for m_t? For one, it is valid only in leading order of $1/N_c$ with $g_3 = 0$. This result, moreover, neglects the full dynamical effects of gauge bosons and the composite Higgs boson, which should be included in the renormalization group running from the scale Λ to low energies below. We note that this result is substantially less than the full Standard Model result as obtained in Section IV.

Analogous results are obtained for the neutral gauge boson masses, but they contain no additional information beyond that described here, a consequence of the conventional $I = \frac{1}{2}$ breaking mode. The only technical challenge in the analysis is that we now have the mixing between the $U(1)$ and neutral $SU(2)$ gauge bosons induced by the difference between the top quark and b–quark masses. We give the full analysis of this in Appendix A. Moreover, the usual ρ parameter relationship for m_t is obtained.

In Appendix B we observe that the evolution of the coupling constants g_1 and g_2 (as seen in eq.(2.14)) is equivalent to that given by the renormalization group for the truncated model in the bubble approximation (*i.e.*, without gauge coupling constants). Thus, the effective Lagrangian at scales below Λ must produce this evolution. We thus turn now to a discussion of the effective Lagrangian.

III. Low Energy Effective Lagrangian

A. Induced Higgs Scalar

In the previous section and Appendices A and B we derived the low energy effects of dynamical symmetry breaking provided by a sufficiently attractive four–fermion interaction involving the top quark as defined in eq.(1.1). We considered a model based on a conventional sum of the fermion bubble diagrams associated with the leading large–N_c limit with $g_3 = 0$. This simple model generates dynamical masses for the top quark and gauge bosons of the Standard Model, as well as a bound state corresponding to the usual physical Higgs scalar of mass $2m_t$. In Appendix B we show that the fermion bubbles yield their conventional contribution to the running of the gauge coupling constants and the explicit cut–off dependence can be absorbed by appropriate renormalization of these couplings. The effective Higgs vacuum expectation value, $v^2(0)$, has the normal isospin structure related to the ρ parameter but remains sensitive to the cut–off Λ as its dependence cannot be absorbed by renormalization. Our calculations imply that the effective low–energy dynamics is, in fact, just the usual Standard Model with certain constraints on the fundamental parameters of the theory.

We can see the connection with the Standard Model by using a Yukawa form of the four–fermion interactions as defined at the cut–off scale Λ, through the help of a static, auxiliary Higgs field, H. We can rewrite eq.(1.1) as:

$$L = L_{kinetic} + g_t(\bar{\Psi}_L t_R H + h.c.) - m_0^2 H^\dagger H \tag{3.1}$$

If we integrate out the field H we produce the four–fermion vertex as an induced interaction with $G = g_t^2/m_0^2$. Note here that $m_0^2 \sim \Lambda^2$, and positive, implies an attractive interaction. For low energy phenomena we may wish to keep the effective Higgs field and integrate out the short distance components of the fermion fields.

The analysis of Section II may be interpreted as implying that at scales below the cut–off, Λ, the Higgs field H develops induced, fully gauge invariant, kinetic terms and quartic interaction contributions in the effective action. Indeed, we can exactly reproduce the results of the previous section if we use the large–N_c limit to compute the fermion loop contributions.

The full induced effective Lagrangian will take the form:

$$\begin{aligned} L &= L_{kinetic} + g_t(\bar{\Psi}_L t_R H + h.c.) + \Delta L_{gauge} \\ &\quad + Z_H |D_\mu H|^2 - m_H^2 H^\dagger H - \frac{\lambda_0}{2}(H^\dagger H)^2 \end{aligned} \tag{3.2}$$

where D_μ is the gauge covariant derivative and all loops are now to be defined with respect to a low energy scale μ. Here ΔL_{gauge} is the usual fermion loop contribution to the renormalization of the gauge coupling constants as given in Section II.C and Appendix B. A direct evaluation of the induced parameters in the Lagrangian gives:

$$\begin{aligned} Z_H &= (4\pi)^{-2} g_t^2 N_c \log(\Lambda^2/\mu^2) \\ m_H^2 &= m_0^2 - (4\pi)^{-2} g_t^2 (2N_c)(\Lambda^2 - \mu^2) \\ \lambda_0 &= (4\pi)^{-2} g_t^4 (2N_c) \log(\Lambda^2/\mu^2) \end{aligned} \tag{3.3}$$

The Lagrangian of eq.(3.2) is exactly the same as the usual low energy Standard Model, except that we are not free to renormalize the two induced parameters, Z_H and λ_0, which must remain log–divergent, *i.e.*, have an explicit dependence upon Λ. The mechanism for spontaneous symmetry breaking is now seen in the effective Higgs mass which is driven by the additive quadratic dependence upon Λ to a finite, negative value by the fermion loop contributions; the bare mass, m_0^2, requires the usual fine–tuning to produce a finite VEV of the Higgs field (or top quark mass).

If we use the above tree–Lagrangian to estimate the physical spectrum of the low

energy theory, we find:

$$\begin{aligned} m_t &= g_t \left\langle H^0 \right\rangle \\ m_H^2 &= 4\lambda_0 \left\langle H^0 \right\rangle^2 / 2Z_H = 4(\lambda_0/g_t^4)m_t^2 = 4m_t^2 \\ v^2 &= m_Z^2/(g_1^2+g_2^2) = \frac{1}{2}Z_H \left\langle H^0 \right\rangle^2 = \frac{1}{2}(Z_H/g_t^2)m_t^2 \\ &= (N_c/2)(4\pi)^{-2} m_t^2 \log(\Lambda^2/\mu^2) \\ &= \bar{v}^2 \end{aligned} \tag{3.4}$$

which agree with the previous results for the divergent parts in Section II; we have previously noted that the running of the gauge coupling constants are as expected in the leading N_c approximation. Full agreement with the previous section's results can be achieved by adding the low energy fermion loop corrections to the results of eq.(3.4).

At this point it is useful to anticipate some of the discussion of Section IV concerning the renormalization group evolution of the quartic Higgs coupling constant. The high energy renormalization group running of the Higgs quartic coupling, λ_0, as seen in eq.(3.3) is consistent with the contribution of a single quark–doublet contribution to the renormalization group equation. The conventional Higgs coupling constant should be identified with:

$$\lambda = \lambda_0 / Z_H^2. \tag{3.5}$$

This satisfies, in the full Standard Model, the one–loop renormalization group equation:

$$16\pi^2 \frac{\partial}{\partial \ln \mu} \lambda = \left\{ 12\lambda^2 + 4N_c \lambda g_t - 4N_c g_t^2 \right\} \tag{3.6}$$

Here the fermion loops contribute the last two terms, and they are seen to follow from combining eq.(3.3) for Z_H and λ_0.

We have seen that the introduction of the four–fermion terms at the scale Λ can be written in terms of the static Higgs field with Yukawa couplings to the fermions. In the large–N_c limit the theory evolves at low energy to a complete Standard Model with a dynamical Higgs field. The appropriate renormalization group equations are just those obtained in the usual Standard Model. The compositeness conditions, $Z_H = \lambda = 0$, are associated with the boundary conditions for the running couplings at the high energy scale Λ. The composite Higgs theory can be identified with entire renormalization group trajectories of the full Standard Model. This statement is exact in the large–N_c limit as we have shown by explicit calculation. We conjecture that this same identification can be made beyond this approximation.

At low energy the Standard Model is not dominated by the fermion loop contributions, and radiative corrections from virtual gauge and Higgs propagation are essential. However, we expect that the renormalization group trajectories for the composite Higgs theory should be associated with the vanishing of Z_H and λ for the full theory just as the normal Landau ghost poles are associated with the existence of composite gauge bosons. Our treatment of the full renormalization group equations is given in Section IV.

B. Generalizations

The dynamical model presented here may be generalized in several directions. First, it is readily seen that the full Standard Model couplings for fermions, including light quarks and leptons, may be incorporated into the structure of the four–fermion Lagrangian. The Yukawa couplings in eq.(3.1) may be generalized to the full set of massive fermions:

$$\begin{aligned} L &= L_{kinetic} + g_{ij}^{+2/3}(\bar{\Psi}_L^i q_R^{j\,(+2/3)} H + h.c.) + g_{ij}^{-2/3}(\bar{\Psi}_L^i q_R^{j\,(-1/3)} H^c + h.c.) \\ & \quad g_{ij\,(l)}(\bar{\Psi}_L^{i\,(l)} q_R^{j\,(l)} H^c + h.c.) - m_0^2 H^\dagger H \end{aligned} \tag{3.7}$$

where $H_i^c = \epsilon_{ij} H^{j\dagger}$. The standard Cabibbo–Kobayashi–Maskawa structure can be readily input. Also, axion and familon degrees of freedom can occur at the generalized level of eq.(3.7). Integrating out the static auxiliary Higgs field produces the fundamental four–fermion interaction.

More general four–fermion interactions may require more than one auxiliary Higgs field which then may also become dynamical at low energies. However, while we can always introduce spectator Higgs doublets into the Standard Model which do not couple to quarks or leptons, all of the composite Higgs bosons must couple to matter fields. Thus, the dynamical mechanism is less general than the Standard Model, *i.e.*, the four–fermion interactions admit a limited number of "square roots." An analysis of the allowed dynamical Higgs bosons will be given elsewhere.

The fermion mass matrices observed at low energy depend upon the specific structure of the four–fermion interactions introduced at high energy, and no obvious simplification occurs from the composite Higgs mechanism. We will return to these issues elsewhere.

IV. Predictions of the Full Standard Model

A. Renormalization Group Boundary Conditions

We have seen in section III that the interaction of eq.(1.1) can be described by an induced auxiliary Higgs scalar. Below the scale Λ the field H acquires gauge invariant kinetic terms and quartic interactions. The dynamical origin of the Higgs field thus implies special boundary conditions on the Higgs-Yukawa and Higgs–quartic coupling constants at the Higgs compositeness scale Λ.

Consider now the Lagrangian of eq.(3.2):

$$\begin{aligned} L &= L_{kinetic} + g_{t0}(\bar{\Psi}_L t_R H + h.c.) \\ &\quad + Z_H |D_\mu H|^2 - m_H^2 H^\dagger H - \frac{\lambda_0}{2}(H^\dagger H)^2 \end{aligned} \tag{4.1}$$

We include here the gauge invariant kinetic terms of the Higgs doublet and its quartic interaction as well as the wave–function normalization constant, Z_H, and the top quark will have its own gauge invariant kinetic terms separately for left– and right–handed fields with wave–function normalization constants Z_{tL} and Z_{tR}.

Conventionally one normalizes the kinetic terms of a field theory at any scale, μ, with a condition that the kinetic terms have free–field theory normalization. That is, we may exercise our freedom of rescaling the various fields, H, Ψ_L, t_R, *etc.*, to define $Z_H = 1$ and $Z_{tL} = Z_{tR} = 1$, *etc.* This is accomplished by, *e.g.*, computing 1PI matrix elements of the kinetic terms treated as local operators and obtaining perturbative expressions for the Z_i, and then absorbing these overall multiplicative factors into the fields, $H \to H/\sqrt{Z_H}$, $\Psi_L \to \Psi_L/\sqrt{Z_{tL}}$, $t_R \to t_R/\sqrt{Z_{tR}}$, etc. The coupling constants, such as $\bar{g}_t$ and $\bar{\lambda}$ are then renormalized as usual:

$$\bar{g}_t = \frac{Z_{HY}}{\sqrt{Z_H Z_{tL} Z_{tR}}} g_{t0}; \quad \bar{\lambda} = \frac{Z_{4H}}{Z_H^2}\lambda_0 \tag{4.2}$$

where Z_{HY} (Z_{4H}) is the proper vertex renormalization constant for the Higgs–Yukawa (Higgs–quartic) interactions, and the "$\bar{}$" will henceforth denote quantities in the conventional normalization conditions.

In the present case, however, the Higgs field is dynamical with a vanishing wave–function renormalization constant at the scale Λ. It is useful, therefore, to adopt an "unconventional" normalization convention which does not set $Z_H = 1$. At the scale Λ we have a finite coupling constant $G = g_t^2/m_H^2$, and we are free to define (though this is not necessary, as it does not affect the auxiliary nature of H at Λ) vanishing λ. That is, we have the following conditions at Λ (in terms of the unconventional normalization):

$$g_t \to \text{constant}; \qquad Z_H \to 0; \qquad \lambda \to 0. \tag{4.3}$$

It is easy to see that the transformation $H \to H/\bar{g}_t(\mu^2)$ with the running Higgs–Yukawa coupling $\bar{g}_t(\mu^2)$ transforms the conventional normalization into that required by eq.(4.3). We thus have:

$$\tilde{Z}_H = \frac{1}{\bar{g}_t^2(\mu^2)} \tag{4.4}$$

$$\tilde{\lambda} = \frac{\bar{\lambda}(\mu^2)}{\bar{g}_t^4(\mu^2)} \tag{4.5}$$

where the "$\tilde{}$" will henceforth denote the normalization convention appropriate for compositeness.

The conditions eq.(4.4) and eq.(4.5) allow us to discuss the compositeness conditions eq.(4.3) in terms of the usual running couplings $\bar{g}_t(\mu^2)$ and $\bar{\lambda}(\mu^2)$ of the Standard Model. It is clear that $\tilde{Z}_H \to 0$ requires $\bar{g}_t(\mu^2)$ to blow up at Λ which can be translated into a condition for the physical top quark mass. We may utilize the full one–loop β-functions (neglecting light quark masses and mixings) of the Standard Model:

$$16\pi^2 \frac{d\bar{g}_t}{dt} = (\frac{9}{2}\bar{g}_t^2 - 8\bar{g}_3^2 - \frac{9}{4}\bar{g}_2^2 - \frac{17}{12}\bar{g}_1^2)\bar{g}_t \tag{4.6}$$

and, for the gauge couplings:

$$16\pi^2 \frac{d\bar{g}_i}{dt} = -c_i \bar{g}_i{}^3 \tag{4.7}$$

with

$$c_1 = -\frac{1}{6} - \frac{20}{9}N_g; \quad c_2 = \frac{43}{6} - \frac{4}{3}N_g; \quad c_3 = 11 - \frac{4}{3}N_g \tag{4.8}$$

where N_g is the number of generations and $t = \ln \mu$.

One can see from eq.(4.6) that once $\bar{g}_t$ is sufficiently large, it will diverge as it evolves to a higher scale. Neglecting the small gauge contributions for sufficiently large $\bar{g}_t$ we have:

$$16\pi^2 \frac{d\bar{g}_t}{dt} = \frac{9}{2}\bar{g}_t{}^3; \quad \text{equivalently,} \quad \frac{d\tilde{Z}_H}{dt} = -\frac{9}{16\pi^2} = const < 0 \tag{4.9}$$

$\tilde{Z}_H$ thus decreases asymptotically with a linear slope in $t = \ln \mu$ and becomes zero at the Landau singularity of $\bar{g}_t(\mu^2)$ at Λ. Although one-loop β-functions do not permit an extrapolation all the way to $\tilde{Z}_H = 0$, a large part of the linear decrease toward the compositeness scale is fully reliable (*e.g.*, $\tilde{Z}_H \gtrsim 0.08$ is within the perturbative regime of $\bar{\alpha}_t \lesssim 1$). Indeed, lattice gauge theory has confirmed that perturbation theory is generally quantitatively reliable in analyzing the initial conditions leading to these fixed-points [6]. This behavior is illustrated by the solid lines of Fig.(4) where the full eqs.(4.6) and (4.7) are used to numerically plot $\tilde{Z}$.

The precise value of the top quark mass will be given by running $\bar{g}_t(\mu^2)$ from very high values at a given compositeness scale Λ down to the mass-shell condition $\bar{g}_t(m_t^2) = m_t/v$. For large $\bar{g}_t$ the β-function eq.(4.6) is positive and changes slope drastically with changes in $\bar{g}_t$. Large initial values for $\bar{g}_t$ at Λ become small if one goes to smaller scales and the nonlinearity focusses a wide range of initial values into a small range of final low energy results. Once $\bar{g}_t$ becomes smaller, the slowly changing gauge couplings are important. For an estimate one can assume that the gauge

couplings are constant which makes clear why the solutions are attracted toward the "effective low energy fixed-point" [4]:

$$\bar{g_t}^2(\mu^2) = \frac{16}{9}\,\bar{g_3}^2(\mu^2) \tag{4.10}$$

In general, the couplings are only evolved over a finite range of t and the effective fixed-point will not always be reached for all initial values. However, for the case of the composite Higgs, as discussed here, the fixed-point is always reached. The action of the effective fixed-point makes the top quark mass prediction very insensitive to the initial high values of the coupling constant close to Λ. Considering $\tilde{Z}_H \to 0$, the uncertainties of higher orders will show up as an uncertainty in the precise position of Λ (see Fig.(4)).

In Table I we give the resulting m_t^{phys} obtained by a numerical solution of the renormalization group equations as a function of Λ. We use $M_Z = 91.8$ GeV and, for the gauge couplings:

$$\bar{g}_1^2(M_Z) = 0.127 \pm 0.009; \quad \bar{g}_2^2(M_Z) = 0.425 \pm 0.006; \quad \bar{g}_3^2(M_Z) = 1.44 \pm 0.19 \tag{4.11}$$

For a different choice of M_Z, the entries in Table I must be rescaled by $M_Z/91.8$ GeV. We calculate errors both from the uncertainties of the experimental input and by varying the initial conditions at Λ. For high Λ the uncertainty in $\bar{\alpha}_3(M_Z)$ dominates the error while for low Λ the errors become bigger due to the use of perturbation theory. The quoted perturbative errors are obtained by varying the top quark mass so that $\bar{\alpha}_t = \bar{g_t}^2/4\pi$ becomes unity at the scale Λ, instead of infinity.

The Higgs boson mass will likewise be determined by the evolution of $\bar{\lambda}$ given by:

$$16\pi^2 \frac{d\bar{\lambda}}{dt} = 12(\bar{\lambda}^2 + (\bar{g_t}^2 - A)\bar{\lambda} + B - \bar{g_t}^4) \tag{4.12}$$

where:

$$A = \frac{1}{4}\bar{g}_1{}^2 + \frac{3}{4}\bar{g}_2{}^2; \quad B = \frac{1}{16}\bar{g}_1{}^4 + \frac{1}{8}\bar{g}_1{}^2\bar{g}_2{}^2 + \frac{3}{16}\bar{g}_2{}^4 \tag{4.13}$$

In Fig. (5) we present the results of numerically integrating eq.(4.12) with the corresponding evolution of $\bar{g}_t$.

To understand the behaviour of the solutions for $\tilde{\lambda}$ it is convenient to define $x = \bar{\lambda}\bar{g}_t{}^{-2}$. The compositeness conditions of eq.(4.3) require that $\tilde{\lambda} = \bar{\lambda}/\bar{g}_4^4 \to 0$ as $\mu \to \Lambda$. Consider eq.(4.12) with $A \approx B \approx 0$:

$$16\pi^2 \frac{dx}{dt} = 12\ \bar{g}_t{}^2\ (x^2 + x/4 - 1) = 12\ \bar{g}_t{}^2\ (x - x_-)(x - x_+) \tag{4.14}$$

$$x_\pm = (-1 \pm \sqrt{65})/8; \quad x_+ \simeq 0.88; \quad x_- \simeq -1.13 \tag{4.15}$$

Since the *rhs* of eq.(4.14) factorizes into $\bar{g}_t{}^2 \times F(x)$, and $\bar{g}_t$ is diverging as we approach Λ, we can see that the variable $x = \bar{\lambda}\bar{g}_t{}^{-2}$ grows faster than $\bar{g}_t{}^2$ for $x > x_+$. Thus $\tilde{\lambda}$ is diverging as it approaches Λ and we cannot fulfill the compositeness conditions on this trajectory. For $x = x_+$ we have an ultraviolet unstable fixed-point, and since the β-function (4.14) vanishes, x remains constant and therefore $\tilde{\lambda} = \bar{g}_t{}^{-2}x_+$. On the other hand, for $x_- \leq x < x_+$, eq.(4.14) shows that x is driven toward the fixed-point x_-. In this case $\tilde{\lambda}$ evolves as $\bar{g}_t{}^{-2}x_-$ and will tend to zero as it approaches Λ. The ratio $\tilde{\lambda}/\tilde{Z}_H$ approaches a constant, indicating that the two quantities do not run independently.

For the physical Higgs mass we have again two mechanisms which make the prediction very stable. If we start with the compositeness condition at Λ then the preceding discussion shows that the ultraviolet unstable fixed-point x_+ becomes attractive as we evolve downwards in scale. This means that $\tilde{\lambda}$ is attracted toward $\bar{g}_t{}^{-2}x_+ = \tilde{Z}_H x_+$. Once the couplings become smaller the effect of the smoothly varying gauge couplings is important which further reduces the sensitivity to the precise initial value at Λ. Thus we conclude that the compositeness condition forces the low energy values close

to the infra-red stable fixed-point. This corresponds to the dashed lines in Fig.(4) and the dash-dotted line (b) in Fig.(5). The resulting Higgs boson masses as a function of Λ are also shown in Table I together with their errors.

It might be noted that the resulting masses correspond to trajectories of $\bar{\lambda}(\mu^2)$ which are positive over most of the range of scale considered. One might be concerned about the possibility that the vacuum is unstable if $\bar{\lambda}(\mu^2)$ becomes negative at any point in the evolution. As one can see from Fig.(5) negative couplings occur only at high scales. They are not necessarily a signature of a phase transition in the effective Lagrangian, since quartic instabilities favor large vacuum expectation values and thus require examination of the full effects of irrelevant operators, *etc.*

B. Phenomenological Constraints

The resulting prediction of the full Standard Model analysis is a top quark mass that might be considered large in comparison to certain published theoretical upper limits. Indeed, it has been claimed that the ρ parameter limit implies $m_t \lesssim 180$ to 200 GeV [7], and this is the most stringent quoted limit. Other constraints follow from $B^0\bar{B}^0$ mixing, and CP-violation, but these are less restrictive and we will ignore them presently. Our principal comments concerning the ρ parameter limit, are as follows:

(i) The quoted limit of Amaldi *et al.* arises from the use of a convolution integral over m_t times a confidence level distribution, which is a function of m_t and $\sin^2\theta_W$. The integral averages over all values of $\sin^2\theta_W$ and m_t. The confidence level distribution derives from comparing the results of deep inelastic neutrino scattering (ν-DIS) [7] to direct determination of M_W and M_Z and $\sin^2\theta_W = A^2/(1-\Delta r)M_W^2$ (as well as the other determinations which have larger errors, are thus of less statistical weight, and may for the purposes of discussion be ignored presently, though they are included

in our figures). Of central importance is the magnitude of the quoted errors of the ν-DIS, as we comment upon below in (ii).

We wish to emphasize that *the derivation of an expected value of m_t by convolution with the confidence level distribution is not the applicable procedure in evaluating the probability that a given theory, which predicts a definite value of m_t, is likely.* In our case, we make no theoretical prediction of $\sin^2\theta_W$, thus we should not integrate over this parameter. Instead, *e.g.*, we have the luxury of asking which value of $\sin^2\theta_W$ maximizes the probability for a given value of m_t, and then using that value of the parameter in evaluating the probability of the given input value of m_t. This is operationally inequivalent to obtaining the bound quoted by Amaldi *et al.* .

We give in Fig.(6) the confidence level contours (a) equivalent to the Amaldi *et al.* results as presented in their Fig.(5). Indeed, $m_t \sim 235$ GeV is allowed at the 95% confidence level. It should be noted from the raw data as presented in Fig.(7) that there is already a signal that the ν-DIS and other results are in slight disagreement, given that $m_t \gtrsim 60$ GeV.

(ii) In fact, recent reexaminations of the quoted errors in ν-DIS suggest that these might be larger than previously thought, by as much as a factor of two [8]. In particular, the QCD slow rescaling parameterization of the dimuon data favors a more liberal error than is used in the Amaldi *et al.* analysis [8] in the parameter m_c, from the previous $m_c = 1.5 \pm 0.3$ GeV to the more liberal 1.3 ± 0.5 GeV. The high statistics of these experiments owes to copious data in the regime where the charm quark is being excited (particularly the narrow band beam CERN experiments), yet no slow rescaling parameterization is perfect below ~ 80 GeV (one can imagine an exclusive analysis of data above 80 GeV in the FNAL wide–band beam which avoids the slow–rescaling region, but would then be statistically limited).

We further emphasize here that *m_c is a parameter in this analysis*, and should not be taken literally as the physical charm mass. This implies an approximate doubling

of the overall ν-DIS errors which drastically reduces its statistical weight as well as shifting the central values down, leading to a lower mean $\sin^2\theta_W$. Moreover, since the radiative correction, Δr [9], is quadratic in m_t for large m_t, this translates into a higher upper limit than previously claimed. To give the reader a feeling for this, we note that upon replacing $m_c = 1.5 \pm 0.3$ GeV by 1.3 ± 0.5 GeV, the ν-DIS data corresponds to the increase in the 90% confidence level $m_t \lesssim 210$ to $m_t \lesssim 260$ GeV. Thus, in Fig.(6) we give the curves (b) representing the confidence level contours for m_t with the liberalized error assumptions. In Fig.(6) we also present the determination sans ν-DIS in curves (c) to give the reader a feeling for its statistical weight in deriving the top quark mass limit.

In the left box of Fig.(7) we have displayed several determinations of $\sin^2\theta_W$ and the combined results from four deep inelastic scattering experiments for two different values of the fitting parameter m_c (1.5 ± 0.3 GeV and 1.3 ± 0.5 GeV). The middle box shows the resulting combined value for $\sin^2\theta_W$ which is then compared with the right box. Note the relatively strong dependence of the result on both m_c and its error due to the change of the central value and statistical weight. In the right box we show $\sin^2\theta_W$ as obtained from $A^2/(1-\Delta r)M_W^2$, and M_W, M_Z. The top quark mass dependence of Δr leads to a different combined result and we show the result for a set of top quark masses (the Higgs mass dependence is very mild and we choose 200 GeV). The last data point shows the range for $\sin^2\theta_W$ from M_W and M_Z alone using the UA-1 and UA-2 combined results (which gives also a bound for m_t). Note that the combined scattering data have a small top quark mass dependence which is not displayed here. Compared to the changes in the right box this is an effect which is roughly 1/6 of the changes in the right box into the opposite direction.

Thus, the oft-quoted stringent limit on m_t hinges crucially upon the experimental errors in ν-DIS when combined with other independent determinations of $\sin^2\theta_W$. It does not appear to be in significant conflict with this data to allow m_t as large as 260

GeV.

(iii) There are preliminary indications from SLC and CDF that the Z^0 mass may be $\sim 1\%$ lower than the central result of UA-1 and UA-2. Though we are unwilling to bet on the ultimate tenability of this result, it should be remarked that this would improve the agreement between ν-DIS and the direct determination for high m_t. In Fig.(7) this corresponds to the upper ends of the ranges of the $\sin^2\theta_W$ predictions from the direct determination with radiative corrections shown in the right box.

In summary, we thus feel that it it is premature to reject predictions of a very heavy top quark, up to at least ~ 260 GeV based upon the present situation in these experiments. Note that, by incorporating the data with our prediction, we favor $\Lambda \gtrsim 10^{13}$ GeV, $\sin^2\theta_W = 0.210$ to 0.220, and the Z^0 mass between 90 GeV and 91.5 GeV. This comes from the fact that the allowed range for $\sin^2\ \theta_W$ becomes smaller for the highest possible top quark masses in Fig. (6). This can be translated directly into a smaller range for M_Z (see *e.g.*[10]). Both SLC and LEP should soon provide absolute measurements of M_Z, and CDF a precise determination of the ratio M_W/M_Z, which can be viewed as consistency tests of this scenario for three generations. Our predictions for $\sin^2\theta_W$ and M_W are conveniently summarized by the following equations:

$$\sin^2\theta_W = 0.215 \pm 0.002 + 0.0067(91.1 - M_Z) + 0.00017(230 - m_t), \qquad (4.16)$$

$$M_W = 80.73 \pm 0.15 + 1.23(M_Z - 91.1) + 0.009(m_t - 230). \qquad (4.17)$$

If, ultimately, the theoretical top quark mass prediction is too high to be consistent with radiative corrections or subsequent measurements of M_W, M_Z, *etc.*, then it is still possible, albeit possibly less compelling, to maintain this mechanism by assuming that the gap equation (2.2) is saturated by a fourth generation. The top quark then plays no important role itself in the symmetry breaking of the Standard Model and should have a mass between current lower bounds, but presumably much less than

the predictions for the masses of the fourth generation. In Table II we present the corresponding predictions for the masses of a degenerate fourth doublet. The resulting modified predictions for the Higgs mass as well as the corresponding errors are also shown.

V. Conclusions

Our principal conclusions are as follows:

(1) The gauged Nambu–Jona-Lasinio mechanism within the framework of the Standard Model, dynamically broken by a strongly coupled top quark which forms a condensate $\langle \bar{t}_L t_R \rangle$, may be implemented in the fermion loop approximation (or large–N_c with vanishing g_3). It yields primitive relationships between M_W and m_t and the cut–off Λ, and the Higgs mass is determined as $m_H = 2m_t$. The latter relationship has been emphasized by Nambu [1]. From our point of view, the relationships obtained in this part of the analysis are crude, but correctly indicate that the low energy effective Lagrangian is the Standard Model with conventional running of coupling constants and with the special compositeness condition, $Z_H \to 0$ as $\mu \to \Lambda$.

(2) We infer that $\tilde{Z}_H \to 0$ as $\mu \to \Lambda$ is the general compositeness condition for the Higgs boson of the full theory. The conventional normalization, $Z_H = 1$, implies, equivalently, that $\tilde{g}_t$ and $\tilde{\lambda}$ diverge as $\mu \to \Lambda$. This constraint, in turn, implies that the low energy values of these coupling constants are controlled by the renormalization group infra–red fixed–points. Consequently, the low energy results are insensitive to the detailed behavior of $\tilde{g}_t$ and $\tilde{\lambda}$ as $\mu \to \Lambda$.

(3) We give our results for the full Standard Model as functions of the scale of new physics (or Higgs boson compositeness scale), Λ. Our favored results for m_t are the lower values, as constrained by phenomenological considerations, hence $m_{top} \approx 230$ GeV and $m_{Higgs} \approx 260$ GeV with $\Lambda \approx 10^{15}$ GeV. The mechanism may be adapted

to a fourth generation, or a multiple dynamical Higgs scheme, though our primary impetus is in the connection with the top quark since the lower mass limits on the top quark are suggestive of a strongly coupled system.

(4) We argue that existing phenomenological bounds on m_t are not yet sufficiently restrictive to rule out this scheme for large scales $\Lambda \gtrsim 10^8$ GeV. We believe, as per the discussion of Section IV.B, that the amended bounds from ρ parameter analysis should be of order $m_t \lesssim 260$ ($m_t \lesssim 280$) GeV at the 90% (95%) confidence level. A better understanding of the ν–DIS experiments could possibly rule out our mechanism involving the top quark dynamics.

As our discussion has indicated, the compositeness of the auxiliary Higgs field leads to predictions for the top quark and Higgs masses which are equivalent to effective fixed–point arguments. There is some confusion in the literature on what these fixed–points really mean. We emphasize that for us, the fixed–point in g_t is that previously considered in [4], and is quite distinct from that originally proposed by Pendleton and Ross [11]. The proposal of Pendleton and Ross focussed upon a relationship between g_{top} and g_3 which causes the ratio of these coupling constants to be fixed for all scales. It is thus a "reduction of coupling constants" in the language of Kubo, Sibold and Zimmermann, [12]. The reduction is really a far–UV constraint, *i.e.*, one assumes that g_t must smoothly go to zero with g_3, hence the rate of change of $\log g_t/g_3$ must vanish asymptotically. Our mechanism is not a coupling constant reduction in this sense, and g_3 only acts to control g_t as we approach the infra–red. Nonetheless, we were driven to consider the infra–red fixed–point from a specific compositeness condition implemented at Λ. We should remark, however, that with respect to $\bar{\lambda}$, the Higgs–quartic coupling constant, our mechanism does involve, in some sense, a reduction of coupling constants from $\bar{\lambda}$ to $\bar{g}_t$ in the sense of [12], but here the couplings are diverging together, rather than approaching zero uniformly. Note that previously fixed–point ideas have been used primarily to give probabilistic values of low energy parameters

irrespective of their the high energy values. We have shown presently that certain renormalization group trajectories actually follow from compositeness constraints. The derived masses are closely related to the limits obtained from "triviality bounds," in particular, for a given scale Λ these are equivalent to the simultaneous uppermost allowed values of m_{top} and m_{Higgs}, [13].

Marciano has recently considered ideas that appear close to those discussed here [14], but in fact differ substantially in implementation and conclusions. In the first part Marciano simply emphasizes the Pendleton–Ross [11, 12] "fixed–point," independently of consideration of dynamical symmetry breaking, and gives improved values using up–to–date input parameters. In the second part of the discussion he considers the Higgs to be composite. Here we are in fundamental disagreement on two points: (i) At scales $\mu << \Lambda$ the physical Higgs boson, with gauge invariant kinetic terms, must appear in the effective action, so the effects of its propagation *should be kept in loops*, hence the full Standard Model with the effects of a point–like Higgs boson in the renormalization group equations are relevant. These effects are neglected in [14]. (ii) The compositeness conditions are *boundary conditions* on $\bar{g}_t$ and $\bar{\lambda}$, following from $\tilde{Z}_H \to 0$ as described here, and not the asymptotic smoothness assumptions implied Marciano's work (effectively as in [11, 12]).

Miransky, *et al.*, [2] have also elaborated Nambu's idea of a top quark condensate driving the breaking of the electroweak interactions, and obtain somewhat different results than those presented here. The authors of [2] focus upon the idea of large anomalous dimensions for the four–fermion interaction which is interpreted as a signal for dimensional transmutation and the occurence of a scalar Higgs boundstate. We do not share this viewpoint. Indeed, the formation of a *low mass* scalar state, and top quark mass term, is fundamentally tied to the fine–tuning of the gap equation which then leads to the large–distance propagating composite particles. Without this fine–tuning it makes no sense to talk about the scalar boson state, as then

the bubble diagrams produce only a perturbative, local renormalization of the four–fermion interaction. Anomalous dimensions refer only to the local, short–distance renormalization effects, and do not have anything to do with large–distance dynamical propagating fields. For example, in QCD we only consider the short–distance gluon radiative corrections as comprising the anomalous dimension of a given operator, *e.g.*, as in the nonleptonic weak interactions, and which may be arbitrarily large; we do not consider the pion propagation to arise as a consequence of, or play a role in the anomalous dimension. Thus, we believe that there is a confusion in ref.[2] of short– and long–distance effects and a lack of discussion of the relevant mechanism which leads to long–distance propagating boundstates, *i.e.*, the fine–tuning of the gap equation (We note that this should not be confused with the mechanism of walking technicolor in which large anomalous dimensions are used justifiably to separate the scales of TC and ETC). The vacuum structure of the low energy theory depends on the fine–tuning of the composite Higgs mass and both symmetric and broken symmetry phases of the theory can only be understood on the basis of the dynamics of the composite Higgs field. Although our general approaches are similar, it is not clear that the work of Miransky, *et al.* , includes the full dynamics of the effective field theory at low energies as required by our analysis. We should further remark that BCS theory has recently been invoked by other authors [16] to conjecture a pattern of quark and lepton masses and mixing angles, an approach that is orthogonal to our attempt to understand dynamical mechanisms of electroweak symmetry breaking.

We have seen that our mechanism favors a large top quark mass, suggesting a correspondingly large value of $\Lambda \sim 10^{15}$ GeV, and a smaller value of $\sin^2\theta_W \sim 0.21$ to 0.22. These results suggest a number of questions for further analysis, including the possible role of Grand Unified Theories, such as Georgi–Glashow $SU(5)$, where our four–fermion interactions could arise from the high energy GUT symmetry breaking. Of course, the gap equation solutions for a low energy electroweak symmetry breaking demands a fine–tuning, equivalent to the usual gauge–hierarchy

problem. Perhaps one is led to a supersymmetric version of this discussion (and we remark that in the case of SUSY-$SU(5)$ the fixed point predictions for m_t do not radically change [15]). Or, the nature of the dynamical breaking may be subtle and possibly a new mechanism can be found to solve the fine-tuning problem which locks G^{-1} into approximate equality with $N_c\Lambda^2/8\pi^2$. It seems to be interesting to explore those theories that will provide the effective interaction of eq.(1.1), which was the starting point for our analysis, with an eye to understanding the origin of the small quark masses and mixing angles.

We will return to these issues in a more extensive analysis elsewhere.

We wish to thank Prof. Y. Nambu for several discussions concerning his work, Prof. R. Bernstein regarding the ρ parameter limits and phenomenology, and Prof. J. Rosner for useful comments.

Appendix A: Fermionic Bubble Approximation

The present discussion shows how the dynamical symmetry breaking mechanism through top quark condensation works in a fermionic bubble approximation in detail. We presently ignore all gauge boson and composite–Higgs boson radiative corrections, keeping only fermion loops.

We first recall the solution to the gap equation for the induced top quark mass. This is indicated as in Fig.(1) and eq.(2.1):

$$m_t = -\frac{1}{2}G\,\langle \bar{t}t \rangle \tag{A.1}$$

$$= 2GN_c m_t \frac{i}{(2\pi)^4}\int d^4l\,(l^2 - m_t^2)^{-1} \tag{A.2}$$

We shall use eq.(A.2) in what follows. The result of evaluating eq.(A.2) with a momentum space cut–off Λ is as given in eq.(2.3).

We consider the sum of scalar bubbles of Fig.(2) generated by the interaction eq.(1.1):

$$\Gamma_s(p^2) = -\frac{1}{2}G - (\frac{1}{2}G)^2 i\int d^4x\; e^{ipx}\,\langle T\;\bar{t}t(0)\;\bar{t}t(x)\rangle_{connected} + ... \tag{A.3}$$

We see that we may formally sum the series to obtain:

$$\Gamma_s(p^2) = -\frac{1}{2}G\left[1 - 2GN_c\frac{i}{(2\pi)^4}\int d^4l\,(l^2 - m_t^2)^{-1}\right.$$

$$\left. -2GN_c(4m_t^2 - p^2)\frac{i}{(2\pi)^4}\int d^4l\,(l^2 - m_t^2)^{-1}((p+l)^2 - m_t^2)^{-1}\right]^{-1} \tag{A.4}$$

Here the second and third terms in the denominator of eq.(A.4) come from a rearrangement of the terms in the numerator of the Feynman loop–integral and a shift of

the the loop momentum for the fermions. We thus see that the first two terms in the denominator of eq.(A.4) cancel by virtue of the gap equation (A.2). Thus, performing the loop integrals we arrive at a result:

$$\Gamma_s(p^2) = -\frac{1}{2N_c}\left[(4m_t^2 - p^2)(4\pi)^{-2}\int_0^1 dx \log\left\{\Lambda^2/(m_t^2 - x(1-x)p^2)\right\}\right]^{-1} \qquad (A.5)$$

Analogously we obtain the results of eq.(2.7) and eq.(2.9).

Turning to the W boson vacuum polarization, we have:

$$\frac{1}{g_2^2}D^W_{\mu\nu}(p)^{-1} = \frac{1}{g_2^2}(p^\mu p^\nu - g^{\mu\nu}p^2) + \frac{i}{2}\int d^4x \ \left\langle T\ \bar{t}_L\gamma_\mu b_L(0)\ \bar{b}_L\gamma_\nu t_L(x)\right\rangle \qquad (A.6)$$

where g_2 is the $SU(2)$ coupling constant. For the T–ordered product we again expand in the interaction Lagrangian of eq.(1.1) and sum the planar bubbles, Fig.(3). We assume the top quark has a mass satisfying eq.(2.3), and the gap equation is satisfied in the loop expansion, which maintains the gauge invariance. Notice that this sum can thus be written in terms of the flavor bubbles evaluated in eq.(2.10):

$$\begin{aligned}
\frac{1}{g_2^2}D^W_{\mu\nu}(p)^{-1} &= \frac{1}{g_2^2}(p^\mu p^\nu - g^{\mu\nu}p^2) \\
&+ \frac{1}{4}\frac{i}{(2\pi)^4}\int d^4p\ \mathrm{Tr}\left[\gamma_\mu(1-\gamma_5)(\not{p}+\not{k})^{-1}\gamma_\nu(1-\gamma_5)(\not{p}+\not{k}-m_t)^{-1}\right] \\
&- \frac{1}{8}\Gamma_F(p^2)\frac{i}{(2\pi)^4}\int d^4l\ \mathrm{Tr}\left[\gamma_\mu(1-\gamma_5)(\not{p}+\not{l})^{-1}(1+\gamma_5)(\not{l}-m_t)^{-1}\right] \\
&\quad \times\frac{i}{(2\pi)^4}\int d^4q\ \mathrm{Tr}\left[\gamma_\nu(1-\gamma_5)(\not{p}+\not{q})^{-1}(1+\gamma_5)(\not{q}-m_t)^{-1}\right]
\end{aligned} \qquad (A.7)$$

An evaluation of these expressions leads to the result:

$$\begin{aligned}\frac{1}{g_2^2}D^W_{\mu\nu}(p)^{-1} &= (p^\mu p^\nu/p^2 - g^{\mu\nu})\left[\frac{1}{g_2^2}p^2\right. \\ &+ p^2 N_c(4\pi)^{-2}\int_0^1 dx\; 2x(1-x)\log\left\{\Lambda^2/((1-x)m_t^2 - x(1-x)p^2)\right\} \\ &- \left. m_t^2 N_c(4\pi)^{-2}\int_0^1 dx\;(1-x)\log\left\{\Lambda^2/((1-x)m_t^2 - x(1-x)p^2)\right\}\right].\end{aligned} \tag{A.8}$$

We see that the overall inverse propagator is transverse, corresponding to a gauge invariant Higgs mechanism. Nonetheless there is a zero for nontrivial momentum, corresponding to the induced W boson mass. From these follow eq.(2.11) to eq.(2.16).

Analogous results are obtained for the neutral gauge boson masses. Presently we consider the inverse propagator of the neutral gauge bosons as a 2×2 matrix of the form:

$$\begin{aligned}\frac{1}{g_i g_j}D^0_{\mu\nu}(p)^{-1} &= \begin{bmatrix} 1/g_2^2 & 0 \\ 0 & 1/g_1^2 \end{bmatrix}(p^\mu p^\nu - g^{\mu\nu}p^2) \\ &+\frac{1}{2}i\int d^4x \begin{bmatrix} \langle T\, j^3_\mu(0)\, j^3_\nu(x)\rangle & \langle T\, j^3_\mu(0)\, j^0_\nu(x)\rangle \\ \langle T\, j^0_\mu(0)\, j^3_\nu(x)\rangle & \langle T\, j^0_\mu(0)\, j^0_\nu(x)\rangle \end{bmatrix}\end{aligned} \tag{A.9}$$

where g_1 is the $U(1)$ coupling constant. Here the currents are the usual $SU(2)$ and $U(1)$ neutral currents in the unmixed basis:

$$j^3_\mu = \bar{t}_L\gamma_\mu t_L - \bar{b}_L\gamma_\mu b_L \tag{A.10}$$

$$j^0_\mu = \frac{1}{3}(\bar{t}_L\gamma_\mu t_L + \bar{b}_L\gamma_\mu b_L) + \frac{4}{3}(\bar{t}_R\gamma_\mu t_R) - \frac{2}{3}(\bar{b}_R\gamma_\mu b_R) \tag{A.11}$$

and the numerical factors in the individual terms of j^0_μ are the $U(1)$ weak-hypercharges.

Again we expand in the interaction Lagrangian of eq.(1.1) and sum the planar bubbles, Fig.(3). This can be evaluated to yield:

$$\frac{1}{g_i g_j} D^0_{\mu\nu}(p)^{-1} = (p^\mu p^\nu/p^2 - g^{\mu\nu}) \left\{ \begin{bmatrix} 1/g_2^2(p^2) & 0 \\ 0 & 1/g_1^2(p^2) \end{bmatrix} p^2 - \begin{bmatrix} 1 & -1 \\ -1 & 1 \end{bmatrix} v^2(p^2) \right\} \tag{A.12}$$

where:

$$\frac{1}{g_2^2(p^2)} = \frac{1}{g_2^2} + \frac{1}{2}(4\pi)^{-2} \int_0^1 dx\ 2x(1-x) \left\{ \frac{4}{3} N_c \log\left\{\Lambda^2/(m_t^2 - x(1-x)p^2)\right\} + \frac{2}{3} N_c \log\left\{\Lambda^2/(m_b^2 - x(1-x)p^2)\right\} \right\} \tag{A.13}$$

and:

$$\frac{1}{g_1^2(p^2)} = \frac{1}{g_1^2} + \frac{1}{2}(4\pi)^{-2} \int_0^1 dx\ 2x(1-x) \left\{ \frac{20}{9} N_c \log\left\{\Lambda^2/(m_t^2 - x(1-x)p^2)\right\} + \frac{2}{9} N_c \log\left\{\Lambda^2/(m_b^2 - x(1-x)p^2)\right\} \right\} \tag{A.14}$$

and, finally:

$$\begin{aligned} v^2(p^2) = {} & \frac{1}{6} N_c (4\pi)^{-2} \int_0^1 dx\ 2x(1-x)p^2 \log\left\{ \frac{m_b^2 - x(1-x)p^2}{m_t^2 - x(1-x)p^2} \right\} \\ & + \frac{1}{2} N_c m_t^2 (4\pi)^{-2} \int_0^1 dx\ \log\left\{\Lambda^2/(m_t^2 - x(1-x)p^2)\right\} \\ & + \frac{1}{2} N_c m_b^2 (4\pi)^{-2} \int_0^1 dx\ \log\left\{\Lambda^2/(m_b^2 - x(1-x)p^2)\right\} \end{aligned} \tag{A.15}$$

Appendix B: Renormalization of Gauge Coupling Constants

We thus see that the gauge couplings are subject to logarithmic evolution between the scales Λ and M_W. We may write the low energy gauge coupling constants from eq.(A.13):

$$\frac{1}{g_2^2(0)} = \frac{1}{g_2^2} + \frac{1}{6}N_c(4\pi)^{-2}\left\{\frac{4}{3}\log\left\{\Lambda^2/m_t^2\right\} + \frac{2}{3}\log\left\{\Lambda^2/m_b^2\right\}\right\} \tag{B.1}$$

and:

$$\frac{1}{g_1^2(0)} = \frac{1}{g_1^2} + \frac{1}{6}N_c(4\pi)^{-2}\left\{\frac{20}{9}\log\left\{\Lambda^2/m_t^2\right\} + \frac{2}{9}\log\left\{\Lambda^2/m_b^2\right\}\right\} \tag{B.2}$$

We also have the running of g_2 from the W boson propagator, eq.(2.14):

$$\frac{1}{g_2^2(0)} = \frac{1}{g_2^2} + N_c(4\pi)^{-2}\int_0^1 dx\; 2x(1-x)\log\left\{\Lambda^2/(xm_b^2 + (1-x)m_t^2)\right\} \tag{B.3}$$

We see that the *high energy* renormalization group running of g_2 implied by the net coefficients of the $\log\Lambda$ in eq.(B.3) and eq.(A.13) is identical. Thus the high energy running in the unbroken phase corresponding to momenta $p^2 >> m_t^2$ will be consistently that given by either of eq.(B.3) or eq.(A.13). Moreover, the high energy running of g_2 is consistent with one generation quark–doublet contribution to the usual β–function:

$$16\pi^2\frac{\partial}{\partial\ln\mu}g_2 = \left\{-\frac{22}{3} + \frac{N_c}{3}n_q + \frac{1}{3}n_l\right\}g_2^3 \tag{B.4}$$

where n_q (n_l) is the number of quark (lepton) doublets. Thus, the coefficient of $\log\Lambda$ in eq.(B.3) or eq.(A.13) corresponds to $n_q = 1$ in the second term on the *rhs* of eq.(B.4).

Similarly, the high energy running of g_1 may be read off from eq.(B.2) and again is consistent with a single quark doublet contribution to the usual renormalization

group equation:

$$16\pi^2 \frac{\partial}{\partial \ln \mu} g_1 = \left\{ \frac{11}{27} N_c n_q + n_l \right\} g_1^3 \tag{B.5}$$

The fact that this is just the normal renormalization group running of these coupling constants from the single iso–doublet of quarks in the Standard Model (neglecting all other contributions, such as gauge boson loops) indicates that the low energy effective Lagrangian at this order is just the Standard Model.

The further renormalization effects below the scale m_t are radiative corrections that show up at low energy, *e.g.*, neutrino scattering for $Q^2 << M_W^2$. These involve, essentially, the extrapolation from the on–shell W and Z masses to the low energy measured $\sin^2\theta_W$ and G_F. Does the model lead to new effects here?

We see that:

$$G_F^{-1} = v^2(0) = \frac{1}{2} N_c (4\pi)^{-2} \left\{ m_t^2 \log\left\{\Lambda^2/m_t^2\right\} + m_b^2 \log\left\{\Lambda^2/m_b^2\right\} \right\} \tag{B.6}$$

and:

$$\begin{aligned} \bar{v}^2(0) &= N_c (4\pi)^{-2} \int_0^1 dx \, \left\{ x m_b^2 + (1-x) m_t^2 \right\} \log\left\{ \Lambda^2/(x m_b^2 + (1-x) m_t^2) \right\} \\ &= v(0)^2 + \frac{N_c}{4} (4\pi)^{-2} \left\{ m_t^2 + m_b^2 - \frac{2 m_t^2 m_b^2}{m_b^2 - m_t^2} \log(m_b^2/m_t^2) \right\} \end{aligned} \tag{B.7}$$

The difference in $\bar{v}(0)^2$ and $v(0)^2$ is just the usual correction to the ρ–parameter due to weak isospin breaking effects. Thus, there are no additional corrections here beyond the usual Standard Model results. This is analogous to well known results of Carter and Pagels [17]

References

1. Y. Nambu, "Bootstrap Symmetry Breaking in Electroweak Unification," Enrico Fermi Institute Preprint, 89–08 (1989).

2. V. A. Miransky, M. Tanabashi, K. Yamawaki, *Mod. Phys. Lett.* **A4**, 1043 (1989);
"Dynamical Electroweak Symmetry Breaking with Large Anomalous Dimension and top quark Condensate," Nagoya Univ. Preprint, DPNU–89–49.

3. Y. Nambu and G. Jona-Lasinio, *Phys. Rev.* **122**, 345 (1961);
W. A. Bardeen, C. N. Leung and S. T. Love, *Phys. Rev. Lett.* **56**, 1230 (1986); and FERMILAB-Pub-89/22-T.

4. C. T. Hill, *Phys. Rev.* **D24**, 691 (1981).

5. C. T. Hill, C. N. Leung, S. Rao, *Nucl. Phys.* **B262**, 517 (1985).

6. I. Montvay, DESY Preprint, DESY 87/077, *Talk Presented at EPS Conf. on High Energy Physics, Uppsala, Sweden,* (1987);
J. Shigemitsu "Renormalized Yukawa Couplings from the Lattice," Argonne Nat.'l Lab. Preprint, DOE/ER/01545-416; *Phys. Lett.* **189B** 164 (1987).

7. U. Amaldi et al., *Phys. Rev.* **D36**, 1385 (1987);
with slightly more restrictive assumptions see also:
G. Costa et al., *Nucl. Phys.* **B297**, 244 (1988).

8. R. Brock, "Deep–Inelastic Neutrino Measurements of $\sin^2\theta_W$," presented at *New Directions in ν Physics at Fermilab,* September, (1988), to be published; also R. Bernstein and G. P. Yeh, private communications. For a recent study by the CCFR collaboration of the slow rescaling parametrization favoring $m_c =$

1.3 ± 0.5 GeV, see:
C. Foudas *et al.* , submitted to Phys. Rev. Lett.

9. A. Sirlin, *Phys. Rev.* **D22**, 971 (1980);
W. Marciano and A. Sirlin, *Phys. Rev.* **D22**, 2695 (1980);
Phys. Rev. **D29**, 945 (1984);
D. Yu. Bardin, S. Riemann and T. Riemann, *Zeit. Phys.* **32C**, 121 (1986);
F. Jegerlehner, *Zeit. Phys.* **32C**, 425 (1986).

10. P. Langacker, W. Marciano and A. Sirlin, *Phys. Rev.* **D36**, 2191 (1987).

11. B. Pendleton and G. G. Ross *Phys. Lett.* **98B**, 291 (1981).

12. J. Kubo, K. Sibold and W. Zimmermann, *Phys. Lett.* **B220**, 191 (1989);
and *Nucl. Phys.* **B259**, 331 (1985).

13. L. Maiani, G. Parisi and R. Petronzio, *Nucl. Phys.* **B136**, 115 (1978);
N. Cabbibo et al., *Nucl. Phys.* **B158**, 295 (1979);
R. Dashen and H. Neuberger, *Phys. Rev. Lett.* **50**, 1847 (1983);
D. J. E. Callaway, *Nucl. Phys.* **B233**, 189 (1984);
M. Lindner, *Zeit. Phys.* **31C**, 295 (1986).

14. W. J. Marciano, *Phys. Rev. Lett.* **62**, 2793 (1989).

15. J. Bagger, S. Dimopoulos, E. Masso, *Phys. Rev. Lett.* 55, 1450 (1985);
ibid. Phys. Rev. Lett. 55, 920 (1985); *Phys. Lett.* **156B**, 357 (1985).

16. P. Kaus, S. Meshkov, *Mod. Phys. Lett.* **A3**, 1251 (1988);
ibid. (erratum), 4, 603 (1989);
H. Fritzsch, Proceedings Europhysics Conference on Flavor Mixing in Weak Interactions, Erice, Italy, (March 1984), L. L. Chau, ed.;
ibid., MPI-PAE/PTH 22/88 (Munich preprint);

ibid., *Proceedings of the 60th Birthday Symposium for M. Gell-Mann* Pasadena, Calif. (Jan. 1989).

17. A. Carter, H. Pagels, *Phys. Rev. Lett.* 43, 1845 (1979).

Figure Captions

Figure 1: Diagrammatic representation of the gap equation.

Figure 2: Bubble sum generated by the four-fermion interaction.

Figure 3: The planar loops contributing to gauge boson propagators.

Figure 4: The renormalization group evolution of the wave-function normalization constant $\tilde{Z}_H$ (solid lines) and quartic coupling $\tilde{\lambda}$ (dashed lines) for three different scales Λ. Initial values of $\tilde{\lambda}$ are chosen to be precisely on the fixed-point. Both quantities go to zero at $\mu = \Lambda$.

Figure 5: The evolution of $\tilde{\lambda}$ for different initial values and $\Lambda = 10^{15}$ GeV. In (a) the initial value is chosen slightly above the fixed-point and $\tilde{\lambda}$ diverges at Λ. In this case the compositeness condition cannot be fulfilled. Case (b) corresponds to evolution on the low energy attractive fixed-point. The cases (c) - (f) show that the low energy result is insensitive to the initial conditions at Λ. $\tilde{Z}_H$ is also plotted as a solid line.

Fig. 6: Allowed regions for m_t and $\sin^2\theta_W$ for three error hypotheses in the ν-DIS experiments. The solid lines (90% CL) and dashed lines (95% CL) are drawn for (a) $m_c = 1.5 \pm 0.3$ GeV (equivalent to Amaldi *et al.* [7] with $m_H \simeq 250$ GeV); (b) $m_c = 1.3 \pm 0.5$ GeV apropos [8]; (c) disregarding deep inelastic scattering data to indicate its statistical weight in the limit on m_t.

Fig. 7: Comparison of $\sin^2\theta_W$ from different experiments with M_W, M_Z and radiative corrections. The left box shows data from different experiments where radiative corrections for $m_t = 45$ GeV and $m_H = 100$ GeV have been included [8]. The middle box shows the combined result which should be compared with M_W, M_Z and radiative corrections displayed in the right box.

Fig. 1

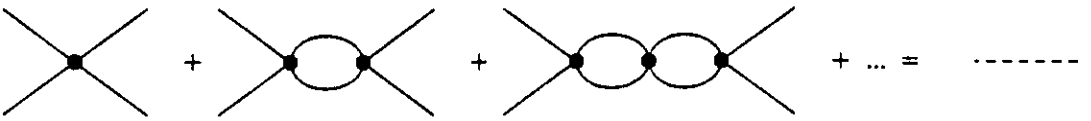

Fig. 2

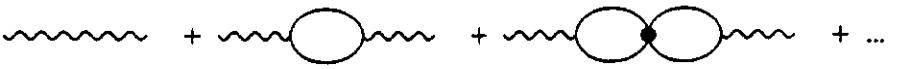

Fig. 3

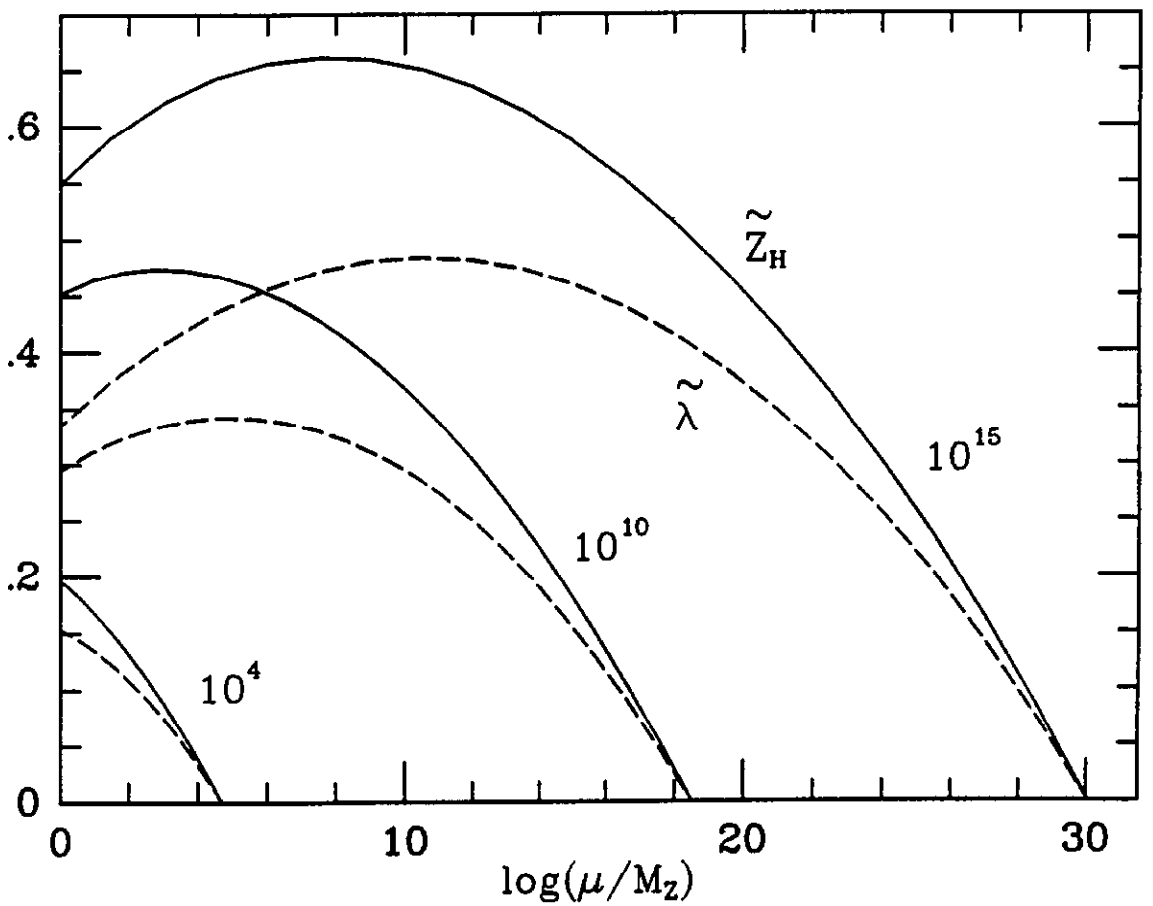

Fig. 4

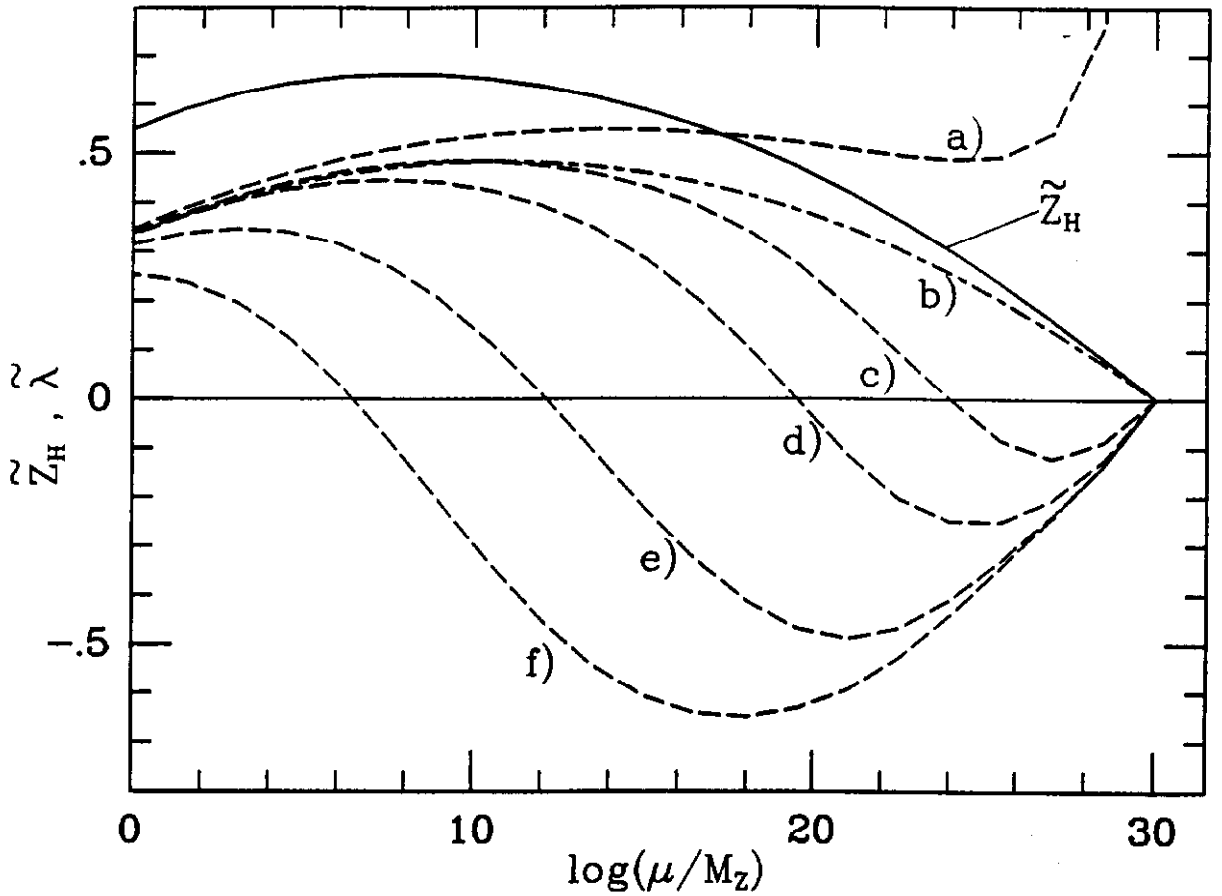
.5
0
-.5
0
10
20
30
$\log(\mu/M_Z)$
$\tilde{Z}_H$
$\tilde{Z}_H$, $\tilde{\lambda}$
a)
b)
c)
d)
e)
f)

Fig. 5

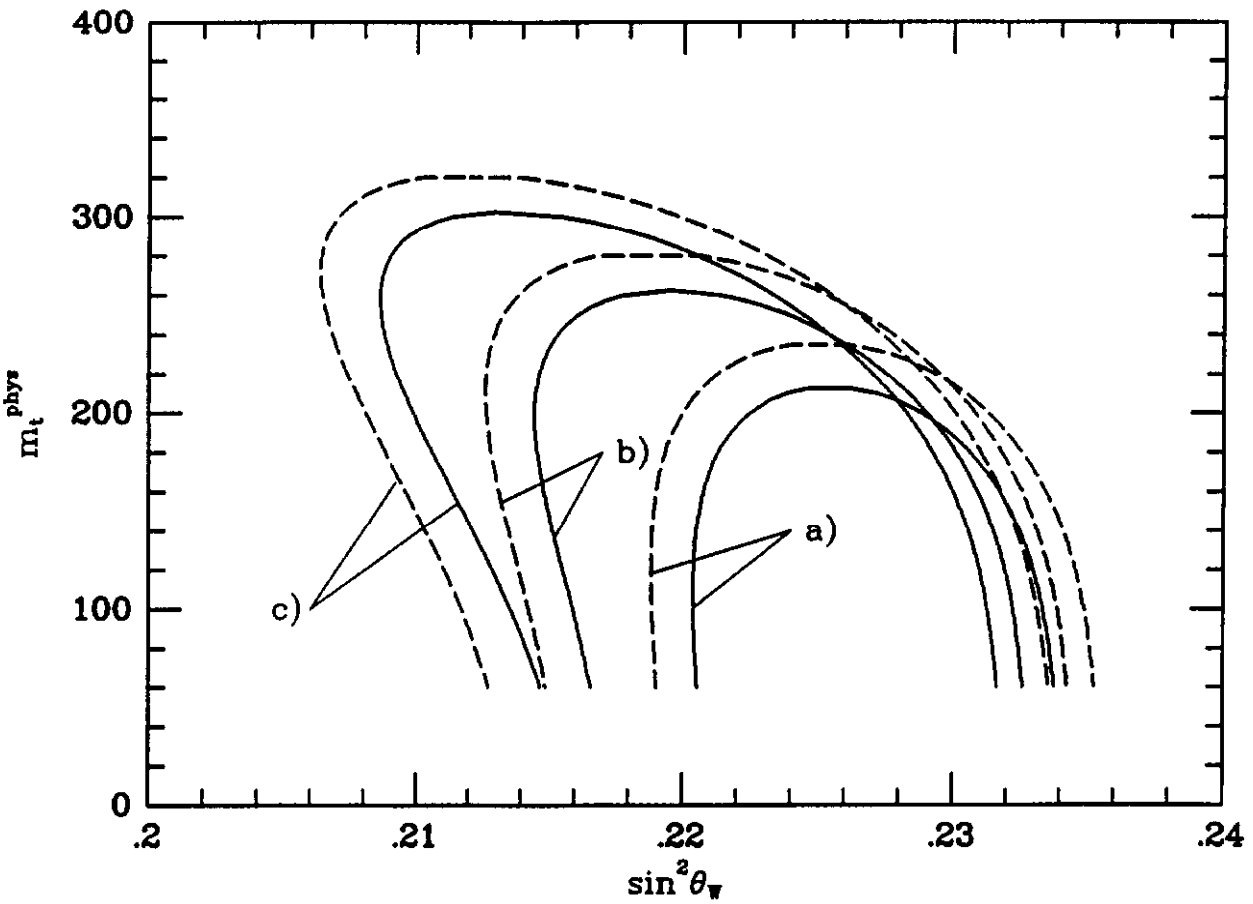
400
300
200
100
0
.2
.21
.22
.23
.24
$\sin^2\theta_W$
m_t^{phys}
a)
b)
c)

Fig. 6

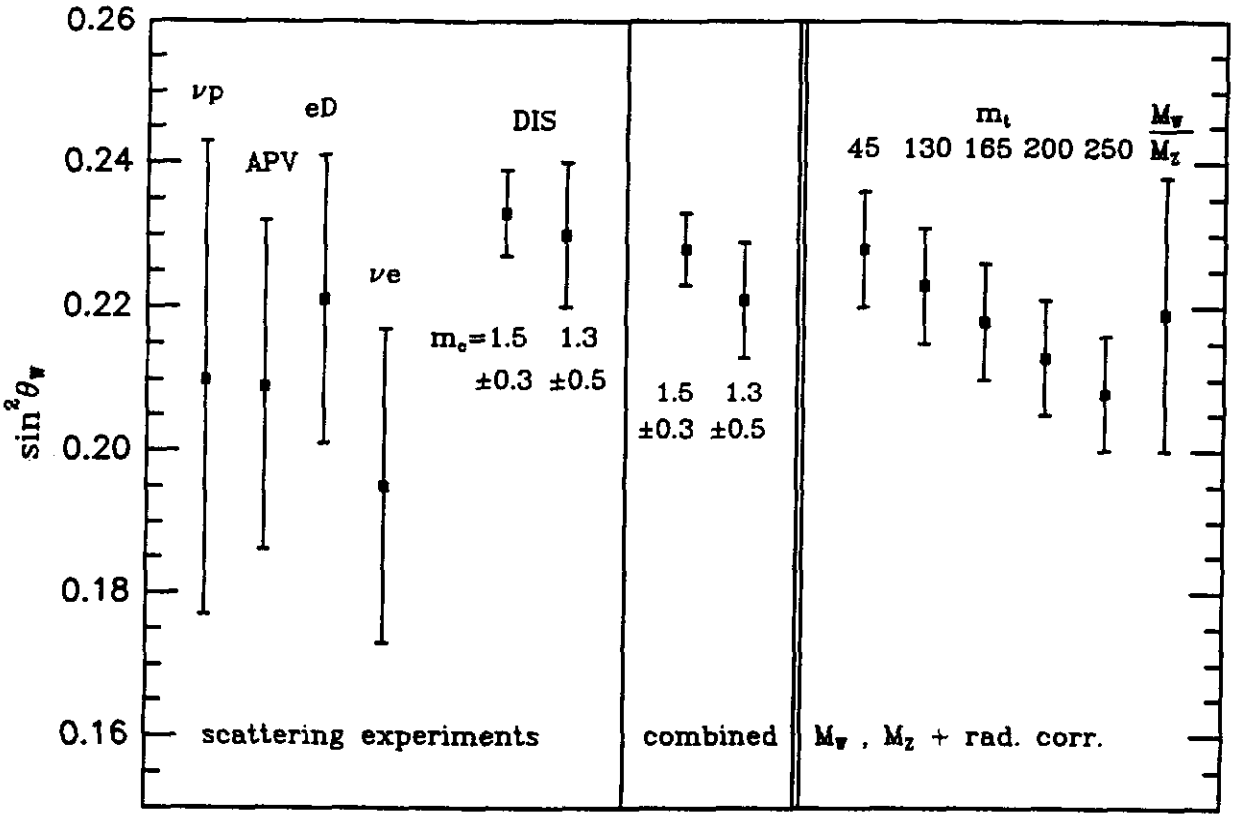
0.26
0.24
0.22
0.20
0.18
0.16
$\sin^2\theta_W$
νp
APV
eD
νe
DIS
m_c=1.5 1.3
±0.3 ±0.5
1.5 1.3
±0.3 ±0.5
m_t
45 130 165 200 250
$\frac{M_W}{M_Z}$
scattering experiments
combined
M_W , M_Z + rad. corr.

Fig. 7

$\Lambda[GeV]$	10^{19}	10^{17}	10^{15}	10^{13}	10^{11}	10^{10}	10^{9}	10^{8}	10^{7}	10^{6}	10^{5}	10^{4}
$m_t^{phys}[GeV]$	220	225	231	239	250	257	266	279	295	320	362	458
pert.	± 2	± 3	± 3	± 3	± 5	± 6	± 7	± 9	± 12	± 16	± 25	± 45
$m_H^{phys}[GeV]$	241	248	258	270	287	298	312	331	356	394	458	609
pert.	± 3	± 3	± 4	± 5	± 8	± 9	± 11	± 15	± 21	± 32	± 56	± 142

Table I: The predictions for the physical top–quark and Higgs boson mass for different scales Λ. One loop β–functions are used with $g_1^2(M_Z) = 0.127 \pm 0.009$, $g_2^2(M_Z) = 0.425 \pm 0.006$, $\alpha_S(M_Z) = 0.115 \pm 0.015$ and $M_Z = 91.8\ GeV$ as input. The numbers are obtained for the central value of these input data and requiring the on-shell condition $\bar{m}(m) = m$. Variation of the gauge couplings within their errors results to a very good approximation in a change of $\pm 6\ GeV$ for the top mass and $\pm 4\ GeV$ for the Higgs mass. The rows labeled *"pert."* show the change in the result if we change the couplings at the cutoff to unity instead of infinity, as a measure of the errors induced by using perturbation theory.

$\Lambda[GeV]$	10^{19}	10^{17}	10^{15}	10^{13}	10^{11}	10^{10}	10^{9}	10^{8}	10^{7}	10^{6}	10^{5}	10^{4}
$m_4^{phys}[GeV]$	200	203	207	213	222	228	235	245	259	279	314	391
pert.	± 1	± 2	± 2	± 2	± 3	± 4	± 5	± 7	± 10	± 14	± 22	± 39
$m_H^{phys}[GeV]$	237	243	250	260	274	284	296	312	335	368	425	557
pert.	± 1	± 2	± 2	± 3	± 4	± 6	± 7	± 10	± 15	± 22	± 39	± 99

Table II: Predictions for a degenerate fourth–generation quark doublet with the same input data as in Table I. The top–quark and the fourth–generation leptons are assumed to be much lighter than this quark doublet. The variation of the gauge couplings results in a change of $\pm 7\ GeV$ for the quark masses and $\pm 5\ GeV$ for the Higgs mass.